Asian Journal of Agriculture and Biology
https://doi.org/10.35495/ajab.2026.044

Original Article

Integrated root leaf metabolomics reveals rootstock specific metabolic syndromes underlying anatomical and growth variation in citrus

Nirmala Friyanti Devy[1], Sri Widyaningsih[1], Farida Yulianti[1], Eriyanto Yusnawan[2], Agus Sugiyatno[1], Siti Subandiyah[3], Hardiyanto[1*]

[1]Research Center for Horticulture, Research Organization for Agriculture and Food, National Research and Innovation Agency of Indonesia. Cibinong Science Center (BRIN), Jalan Raya Bogor, KM. 46, Cibinong, West Java, Indonesia
[2]Research Center for Food Crops, Research Organization for Agriculture and Food, National Research and Innovation Agency of Indonesia. Cibinong Science Center (BRIN), Jalan Raya Bogor, KM. 46, Cibinong, West Java, Indonesia
[3]Department of Entomology and Plant Pathology, Universitas Gadjah Mada (UGM), Yogyakarta, Indonesia

Corresponding author's email: hardiyanto85@yahoo.com
Received: 11 February 2026 / Revised: 05 May 2026 / Accepted: 19 May 2026 / Published Online: 06 June 2026

Abstract

Citrus rootstock selection is usually based on physiological or anatomical characteristics, which restricts integrative knowledge and lowers the efficacy of selection techniques. The lack of cross-organ metabolic evidence further constrains the use of metabolomics in practical rootstock evaluation. This study determined whether coordinated root and leaf metabolomic profiles distinguish five citrus rootstocks and explain variation in leaf anatomy and vegetative growth of *Citrus reticulata* Blanco cv. Keprok Batu 55 (KB) and *Citrus sinensis* L. cv. Manis Pacitan (MP) under highland conditions. Untargeted GC–MS metabolomics, combined with multivariate analysis, anatomical traits, and growth measurements, showed that rootstock identity was the dominant source of variation, with PC1 explaining ~40–45% of the total metabolic variance across organs. Salam and Cleopatra mandarin were enriched in terpenoids, coumarins, and phenylpropanoid-related metabolites, reflecting a defense-associated metabolic profile, whereas Volkameriana and Rough Lemon had a higher relative abundance of intermediates of carbohydrate metabolism, NAD-related compounds, and antioxidants, consistent with a growth-associated profile. Those metabolic configurations are correlated with footsteps in lamina thickness, palisade development, stomatal density, and vegetative growth, all significant at $p < 0.05$. This study is novel in showing root-leaf metabolomic coordination associated with anatomical plasticity and growth variation, and in providing systematic evidence of rootstock-defined metabolic syndromes co-modulated between roots and leaves in tropical citrus systems. These findings highlight the potential of metabolome-informed approaches to support early rootstock pre-selection, pending validation with replicated metabolomic designs.

Keywords: Citrus, Rootstock–scion interaction, Metabolomics, Metabolic syndromes, Leaf anatomy, Growth–defense trade-off

How to cite this article:

Devy NF, Widyaningsih S, Yulianti F, Yusnawan E, Sugiyatno A, Subandiyah S and Hardiyanto. Integrated root leaf metabolomics reveals rootstock specific metabolic syndromes underlying anatomical and growth variation in citrus. Asian J. Agric. Biol. 2026: e2026044. DOI: https://doi.org/10.35495/ajab.2026.044

Introduction

Citrus production in Indonesia spans approximately 55,000 ha with an annual yield of 2.55 million tons; however, productivity remains below global benchmarks (≈35 t ha^{-1} vs. 45–50 t ha^{-1}) (BPS, 2023). One key structural constraint underpinning this gap is that Japansche Citroen (JC; Citrus × limonia), a rootstock which has been shown to substantially increase the profitability of citriculture, remains essentially monodominant across diverse agroecological conditions. If the JC is undeniably the most widely used due to its ease of propagation and broad adaptability, other rootstocks have proven better adapted to highland conditions and exhibit greater drought tolerance (Balfagón et al., 2022; Devy et al., 2023). In addition, the narrowed rootstock base makes them susceptible to huanglongbing (HLB), a phloem-restricted bacterium that currently threatens citrus yields and lifespan across several continents (Tardivo et al., 2025). Diversity in rootstock is therefore a high priority to achieve productivity, resilience, and sustainability in Indonesian citriculture.

In citrus, rootstock-scion interactions are related to water relations, mineral nutrition, and vegetative vigor (Vives-Peris et al., 2023; Wang et al., 2025). To date, the most popular rootstock types, e.g., Cleopatra mandarin, Rough Lemon Volkameriana, and *Poncirus trifoliata* that have powers of salinity tolerance-disease resistance abilities, and adaptability to soil stress conditions (Wang et al., 2020; Bennici et al., 2021). The modulated effects are mediated mainly by long-distance signaling networks, including hormonal fluxes, hydraulic conductance, carbon partitioning, and antioxidant systems from roots to shoots (He et al., 2023; He et al., 2024; Asif et al., 2025; Zhou et al., 2022; Xie et al., 2025; Razi et al., 2024). Plants exhibit an array of integrated physiological and biochemical responses to environmental stress, including but not limited to osmotic adjustment, activation of antioxidant defense mechanisms, and long-distance signaling (Liu et al., 2017; Franco-Navarro et al., 2025).

Recent advances in metabolomics have provided new opportunities to characterize these integrative processes. Rootstock identity has been shown to dramatically influence the composition of both primary and secondary metabolites, including carbohydrates, organic acids, amino acids, phenylpropanoids, flavonoids, terpenoids and coumarins (all of which play an important role in osmotic adjustment, antioxidant defense and plant signaling) using untargeted metabolomic analyses (Maciá-Vázquez et al., 2024; Yang et al., 2024; Morade et al., 2025). In fact, multi-omics studies have shown that rootstocks can differentially modulate specific organ-dependent biosynthetic pathways, e.g., flavonoid and terpene metabolism (Fan et al., 2023). Concomitant with the above, scion–rootstock combinations have also been observed to affect leaf anatomical traits, such as lamina thickness and stomatal density, both of which are directly related to photosynthetic efficiency and stress adaptability (Mesquita et al., 2016; Oustric et al., 2021).

Even with these improvements, a major gap remains. Many of the earlier works have either characterized metabolomic, anatomical, or physiological responses in isolation and/or focused on a single organ (usually leaves or fruits), generally under stress-induced settings. This raises the question of whether rootstocks establish a coherent, cross-organ metabolic organization that is constitutively expressed in roots and leaves, and whether such organizations are systematically coupled to plasticity (movement) and vegetative growth. Previously, drought-induced physiological and molecular responses of Indonesian cultivars such as *Citrus reticulata* cv. Keprok Batu 55 and *C. sinensis* cv. Manis Pacitan has been reported (Devy et al., 2023), but an integrated assessment of metabolome coordination across organs under baseline conditions is missing. This limited integration hinders mechanistic insights and metabolome-informing strategies of rootstock choice with respect to complex constraints, including HLB pressure (Warschefsky et al., 2016; Tardivo et al., 2025)

In that regard, we present rootstock-associated metabolic syndromes, conceptualizing them as cross-organ concordances of organ-specific metabolomes that link coordinated root-to-leaf anatomical and growth characteristics. Addressing this integrative understanding will shift the current paradigm of rootstock evaluation from a trait-based system to a more holistic approach.

Accordingly, we hypothesized that contrasting citrus rootstocks are associated with distinct metabolic syndromes expressed across both roots and leaves, and that these coordinated metabolic patterns correspond to variation in leaf anatomy and vegetative growth. To test this hypothesis, we evaluated five rootstocks (Japansche Citroen, Rough Lemon, Volkameriana, Cleopatra mandarin, and Salam) grafted with two Indonesian scions (Keprok Batu 55 and Manis

https://doi.org/10.35495/ajab.2026.044

Pacitan) using GC–MS-based untargeted metabolomics, multivariate analysis, leaf anatomical measurements, and vegetative growth assessment. The study delivered targeted aims as follows:(i) assess if rootstocks generate their own unique non-leaf specific and reproducible metabolomic profiles in disparate leaves and roots; (ii) unveil the major contributing metabolite classes whose concentrations underlie rootstock differentiation; and (iii) evaluate how closely these metabolomic profiles relate to measured variance in leaf anatomical attributes and vegetative growth across scion–rootstock combinations. Given that metabolomic analyses were conducted on pooled samples, the results are interpreted as exploratory and hypothesis-generating rather than inferential.

Material and Methods

Study site, plant materials and experimental design

This experiment represents an independent study conducted under non-stress highland conditions and is not a continuation of previously published drought experiments (Devy et al., 2023). While similar scion cultivars were used, the present work specifically focuses on rootstock-associated variation, integrating metabolomic, anatomical, and growth traits under baseline conditions.

This study was conducted from February 2023 through August 2024 in a highland citrus research facility at Dau, Malang, East Java (7°56′ S; 112°35′ E; 900 m a.s.l.). Plants were grown in shade house (with a 50–60% reduction in light). Climatic data such as rainfall and temperature were retrieved from the Indonesian Agency for Meteorology, Climatology and Geophysics (BMKG) station (Malang). Mean annual rainfall was in the range 1,800–2,200 mm year^{-1} with a wet season (November to March) and a generally drier period (April to October). Mean annual temperature is 18–24°C, with daily minimums of ~15°C and maximums of 28 °C.

Two commercially important Indonesian citrus scions were evaluated: *Citrus reticulata* cv. Keprok Batu 55 (KB55) and *Citrus sinensis* cv. Manis Pacitan (MP). Five contrasting rootstocks were compared: Japansche Citroen (JC; *Citrus* × *limonia*), Rough Lemon (RL; *C. jambhiri*), Volkameriana (*C. volkameriana*), Cleopatra mandarin (CM; *C. reshni*), and Salam (*Fortunella japonica*). Budding (T-method) was performed on one-year-old rootstocks in January 2022 at the Indonesian Citrus and Subtropical Fruit Research Institute.

One-year-old budding) budded plants were transplanted into 30-L polyethylene bags containing a homogeneous soil:sand:compost (2:1:1 v/v) substrate. The soil showed sandy loam texture, a pH of 6.4 ± 0.2, and a moderate organic carbon content (1.59 ± 0.01%), which were within the ranges of key soil functional controls known to shape the spectral signatures of soils (Zhu et al., 2024). The concentrations of nutrients were: available P_2O_5 (707 ± 196 mg kg^{-1}), total N (0.22 ± 0.06%), exchangeable Ca^{2+} (5.41 ± 0.91 cmol(+) kg^{-1}), and exchangeable K^+ (0.84 ± 0.15 cmol(+) kg^{-1}). Other important soil properties were CEC (18–22 cmol(+) kg^{-1}), exchangeable Mg^{2+} (1.2–1.8 cmol(+) kg^{-1}), low exchangeable Na^+ (<0.3 cmol(+) kg^{-1}) and electrical conductivity < 1 dS m-ı together with micronutrients (Fe, Zn, Mn, B) commonly found in tropical soils and also reached values that are within the normal ranges for this type of soils.

The experiment was a randomized complete block design (RCBD) of 3 blocks. There were two scions × rootstock combinations per block (10 treatment combinations; n = 90 plants), with three biological replicates per treatment within each block. Field-capacity substrate moisture was maintained at ~30% through irrigation, applied twice weekly. Fertilization is NPK (15:15:15, 2 g plant^{-1} month^{-1}).

Sample collection

Sampling took place in August 2024 (18 months post-transplanting; 31 months post-budding) between 07:00 and 09:00 in order to reduce diurnal variation. We sampled fully expanded leaves at mid-canopy positions, and we excavated roots.

For metabolomics, tissues were pooled by mass across biological replicates (10 g fresh weight) to generate composite samples representing treatment-level profiles. In contrast, anatomical and growth measurements were conducted on individual plants to allow statistical inference.

Metabolomic profiling

Extraction and GC–MS analysis

Leaf metabolite extraction followed Hazrati et al. (2022) with modifications. 100 mg of tissue powder was extracted in methanol, sonicated, macerated at 4°C, and derivatized as described by Putra et al. (2024). Root extraction involved ethanol-based maceration of dried powder. Samples were analyzed

https://doi.org/10.35495/ajab.2026.044

using GC–MS (TRACE™ 1310 GC coupled with ISQ™ LT MS, Thermo Fisher Scientific) equipped with an HP-5MS UI column. Operating conditions were as in Abadie et al. (2022).

GC–MS quality control procedures were implemented, including instrument calibration before analysis, consistent retention time alignment using internal standards, and verification of peak reproducibility across samples. Metabolite identifications were performed based on spectral matching against NIST and Wiley libraries with similarity scores ≥80%; ambiguous identifications were filtered out before downstream interpretation.

Multivariate and pathway analysis

Data processing was performed using MS-DIAL, and statistical analyses were conducted in R (v4.3.2). PCA (prcomp) was applied to scaled data, and clustering used Euclidean distance with Ward's linkage (pheatmap package).

Metabolic dissimilarity was assessed using Euclidean and Bray–Curtis indices (vegan package). Pathway enrichment analysis was performed in MetaboAnalyst 6.0 using KEGG, with FDR-adjusted $p < 0.05$ and pathway impact >0.1.

Root metabolites lacking KEGG annotation were classified into functional chemical groups and analyzed descriptively.

Anatomical characterization

General leaf anatomical preparation and staining followed Metusala (2017) and Paul et al. (2017). Morphometric data (lamina thickness, palisade layer, epidermis) were acquired by ImageJ.

Stomatal density was determined using the nail polish method (Auliya et al., 2019), with standardized sampling and imaging.

Growth measurements

Vegetative growth parameters were measured 18 months post-transplanting (August 2024) on three plants per treatment. Plant height (cm) was measured from the soil surface to the apical meristem of the longest vertical shoot using a metric measuring tape. Stem thickness (mm) was recorded at two points using a digital caliper® (resolution 0.01 mm): scion thickness, which was measured at 5 cm above the bud junction on the plant main stem; and rootstock thickness, measured at 5 cm below the bud union. Plants were removed from planter bags, and roots were washed free of substrate with tap water, then rinsed in deionized water for biomass determination. The entire plant was divided into the shoot (above-ground, comprising leaves, stems, and branches) and the root (below-ground, including taproots and lateral roots).

Statistical analysis

Growth, anatomical, and stomatal density data were analyzed using a two-way factorial ANOVA with scion (2 levels) and rootstock (5 levels) as fixed factors and block (3 levels) as a random factor. The interaction between scion and rootstock (scion × rootstock) was explicitly tested and interpreted when significant.

Prior to analysis, data were tested for normality (Shapiro–Wilk) and homogeneity of variance (Levene's test). When necessary, data were transformed ($\log_{10}$ or square-root) to meet ANOVA assumptions.

In addition to p-values, effect sizes (partial eta squared, η^2) were calculated to quantify the magnitude of treatment effects. Post hoc comparisons were performed using Tukey's HSD test ($\alpha = 0.05$).

Because metabolomic datasets (both leaf and root) were generated from pooled biological samples (composite tissues from multiple plants per treatment) without replication, statistical inference was not performed. Therefore, metabolomic results are interpreted as exploratory and descriptive, focusing on multivariate ordination, distance-based dissimilarity metrics (Euclidean and Bray–Curtis), and pathway-level trends rather than univariate statistical testing.

These distance-based metrics appear here as effect-size descriptors of metabolomic separation between treatments and should not be confused with formal hypothesis tests. This is in line with standard plant metabolomics practices, which highlight biologically important signals while diminishing technical variance using pooled sampling (Lisec et al., 2006).

Results

Rootstock effects on leaf metabolomic profiles

Overall variation in leaf metabolomes

Principal Component Analysis (PCA) of leaf metabolomes revealed that the primary axis of ordination (Dim1) accounted for approximately 40–45% of total variance in both *Citrus reticulata* Blanco cv. Keprok Batu 55 (KB55) and *Citrus sinensis* L. cv. Manis Pacitan (MP) (Fig. 1a, b). Dim1 was associated with carbohydrate-related metabolites, sterols, and

organic acid/lactone derivatives—compound classes linked to carbon allocation and membrane-associated metabolism. A second axis (Dim2) was associated with phenolics, terpenoids, and NAD-related pyridines—compound classes. These PCA axes are exploratory summaries of multivariate variance. No formal significance testing was applied to the pooled dataset.

Across all scion–rootstock combinations, eight major biochemical classes were consistently detected in leaf metabolomes: carbohydrates, organic acids/lactones, sterols, phenolics, terpenoids, amino acid–related compounds, NAD-related pyridines, and alkaloids/N-heterocycles (Fig. 1c, d). The consistent representation of all eight classes across treatments indicates that budding establishes a broadly conserved metabolic framework in citrus leaves, regardless of specific rootstock or scion identity. Nonetheless, the relative weighting of these classes in the ordination space differed markedly among cultivar–rootstock combinations, which is reflected in the rootstock-correlated clustering described above.

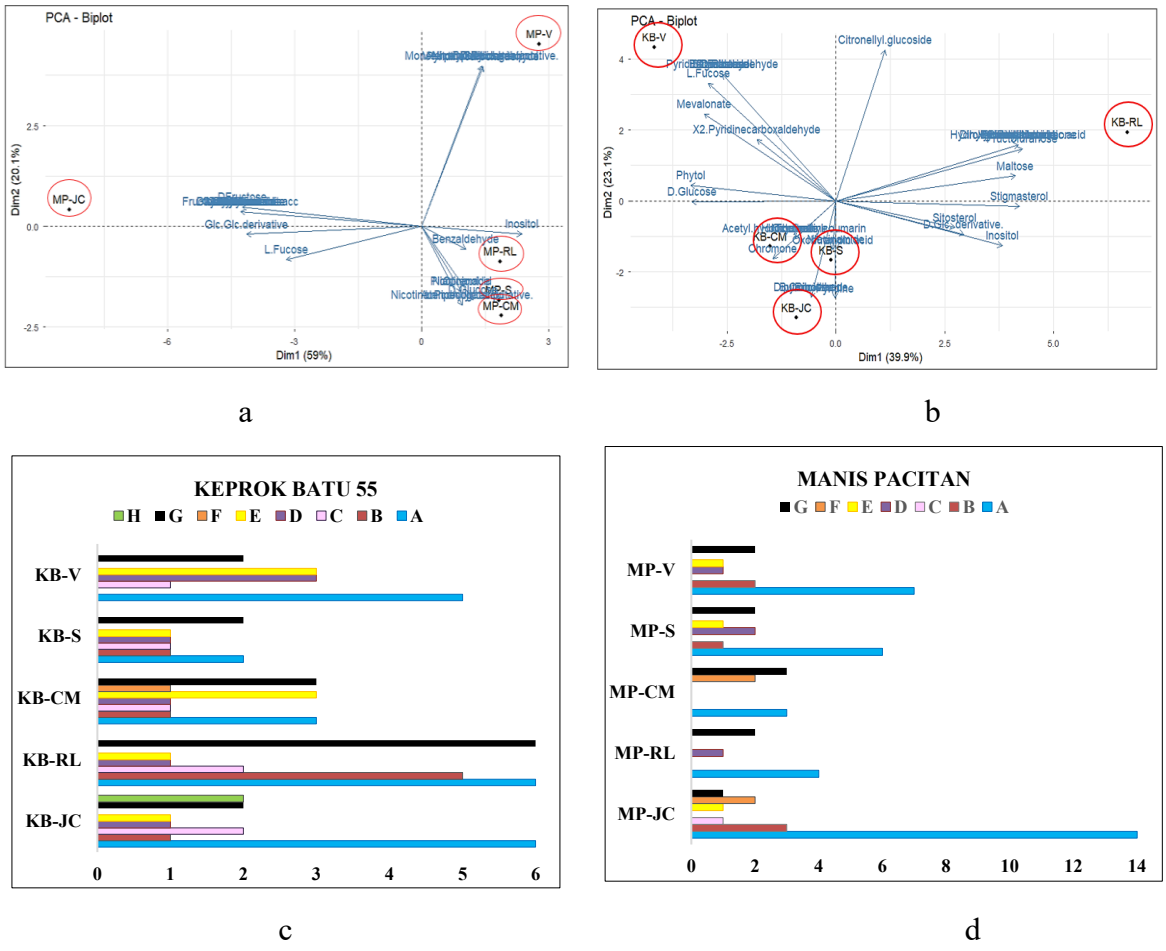

Figure-1. PCA analysis of biological metabolites for cultivar of Keprok Batu 55 (a) and Manis Pacitan (b); and the relative abundance of eight major metabolite classes in leaves of *Citrus reticulata* cv. Keprok Batu 55 (c) and *Citrus sinensis* cv. Manis Pacitan (d) budded onto five rootstocks (JC, RL, CM, S, V); Notes: Metabolites were classified into: A = Sterols; B = Sugars/Carbohydrates; C = Organic acids & lactones; D = Phenolics; E = Terpenoids; F = Amino-acid derivatives; G = NAD-related pyridines; H = Alkaloids/N-heterocycles. The first two dimensions capture gradients of carbohydrate versus redox-associated metabolism (Dim1) and terpenoid/phenolic investment (Dim2).

https://doi.org/10.35495/ajab.2026.044

Key metabolite classes differentiating rootstocks

Inspection of metabolite contributions to PCA axes provided further insight into the biochemical basis of rootstock-correlated variation in leaf metabolomes (Figure 2a, b). Across both cultivars, sugar derivatives (including glucose derivatives, mannobiose, and cellobiose), organic acid/lactone derivatives, and sterols collectively dominated the primary discriminant space, consistent with the interpretation that carbon allocation and membrane-associated metabolism represent a shared biochemical core of rootstock-associated metabolic patterning in citrus leaves.

Cultivar-level differences in contributing metabolite classes were also apparent. The major contributing classes in KB55 were sterols, chromone- and coumarin-related phenolics, and terpenoid-linked compounds, indicating that this isolate is likely undergoing strong structural metabolism as well as secondary defense metabolism. KB55 revealed significant increases in phenolic, terpenoid, and sterol in the relative abundance under JC and RL rootstocks. In MP, the key drivers appeared to be NAD-related pyridines, carbohydrates, and organic acids associated with redox biology, consistent with their established regulatory roles in energy homeostasis and oxidative equilibrium. In response to the CM and V rootstocks, MP demonstrated greater differential modulation of carbohydrate- and NAD-pyridine-class metabolites. The metabolite class composition is, at least partly, sufficient to explain the boundaries between cultivars as determined by PCA in Section 1.1 and supports a common rootstock-associated framework of means for cultivar-specific metabolic emphases. As these observations derive from exploratory multivariate analysis of pooled samples, they should be regarded as hypotheses for targeted future investigation.

Pathway-level patterns in leaf metabolism

Pathway enrichment analysis using KEGG annotations indicated that rootstock-associated differences in leaf metabolomes were distributed across multiple metabolic modules in both cultivars (Figure 2c, d; Table 1). In KB55, the most responsive pathways were concentrated in carbohydrate metabolism—starch and sucrose metabolism, fructose and mannose metabolism, galactose metabolism, amino sugar and nucleotide sugar metabolism, and the pentose phosphate pathway—alongside nicotinate–nicotinamide metabolism and steroid biosynthesis, consistent with coordinated modulation of carbon allocation, redox balance, and membrane-associated metabolism. In MP, pathway associations were more strongly concentrated in carbohydrate metabolism; galactose metabolism, starch and sucrose metabolism, amino sugar and nucleotide sugar metabolism, and fructose and mannose metabolism were the most prominently associated modules, consistent with the higher relative abundance of carbohydrate-class metabolites in this cultivar.

Additional pathways were observed at lower enrichment levels in a cultivar-associated manner. In KB55, vitamin B6 metabolism, butanoate metabolism, thiamine metabolism, glycolysis/gluconeogenesis, and porphyrin metabolism were also represented, albeit with weaker enrichment signals. In MP, weaker associations included fatty acid biosynthesis, lysine degradation, and one-carbon metabolism via folate. Although not at primary enrichment thresholds, these cultivar-associated pathway signals are consistent with additional layers of metabolic specialization superimposed on the conserved carbohydrate core. They should be treated as exploratory observations pending replication with individually replicated samples (Table 1).

Taken together, the leaf metabolomic data present a hierarchical picture of metabolic organization: rootstock identity is broadly associated with a conserved carbohydrate-centered pathway scaffold, while scion genotype is associated with differential weighting of secondary metabolic and regulatory networks within that scaffold. These patterns are summarized in Table 1.

https://doi.org/10.35495/ajab.2026.044

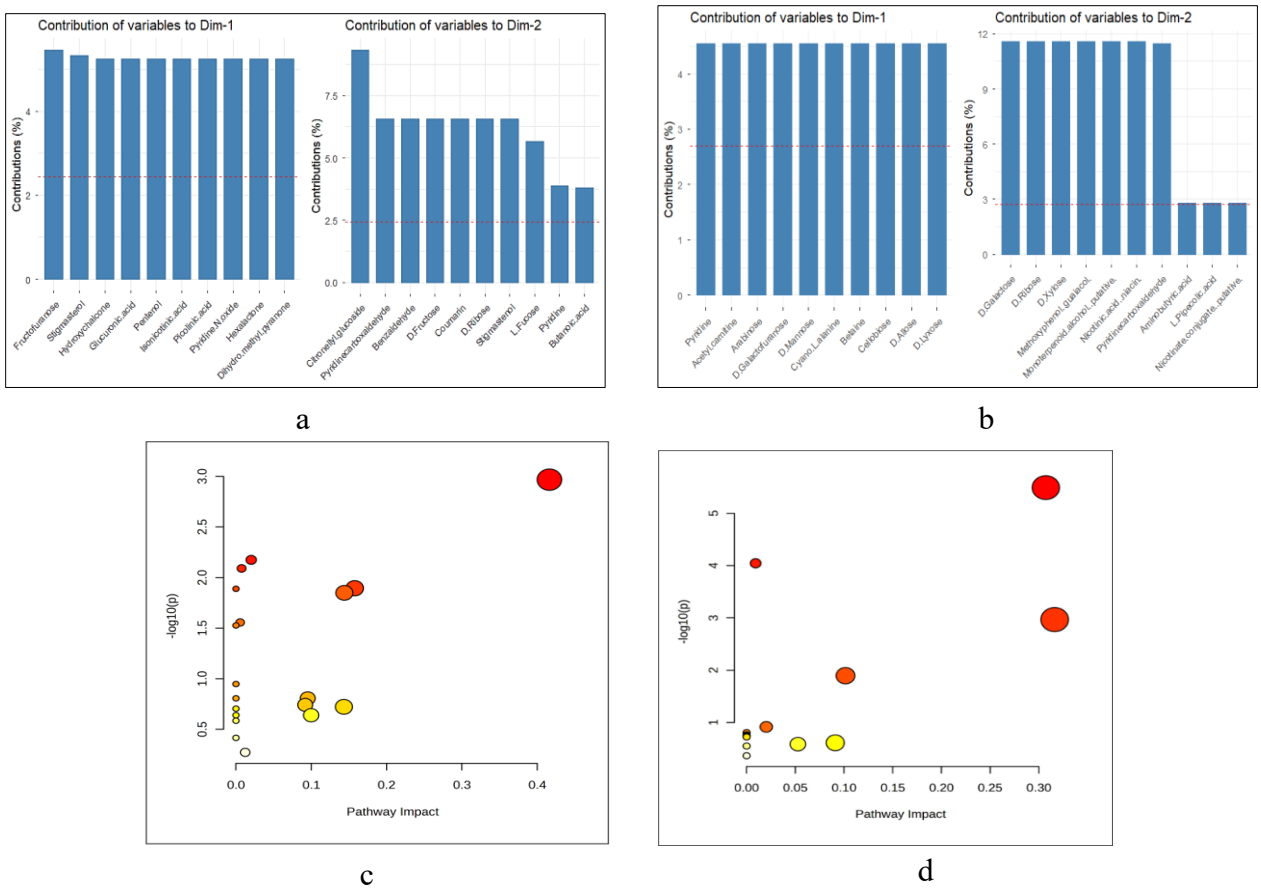

Figure-2. Key metabolite contributions and pathway-level reorganization of citrus leaf metabolism. The relative contribution of discriminant metabolites to Dim1 and Dim2 of the PCA for *Keprok Batu 55* (a); *Manis Pacitan* (b); rootstock-dependent modulation of major metabolic modules in *Citrus reticulata* cv. Keprok Batu 55 (c) and *Citrus sinensis* cv. Manis Pacitan (d).

Table-1. Summary of key metabolic pathway patterns underlying rootstock-driven reprogramming of citrus leaf metabolism.

Pathway category	Keprok Batu 55	Manis Pacitan	Biological interpretation
Core shared pathways	Starch & sucrose metabolism; Galactose metabolism; Fructose & mannose metabolism; Amino sugar & nucleotide sugar metabolism; Pentose phosphate pathway	Same set	Conserved scaffold for carbon allocation and redox buffering imposed by rootstocks
Dominant cultivar-biased pathways	Steroid biosynthesis; Nicotinate–nicotinamide metabolism	Galactose metabolism; Starch & sucrose metabolism	Differential prioritization of membrane stabilization (KB55) vs. carbohydrate flexibility (MP)
Secondary signals (weaker enrichment)	Vitamin B6 metabolism; Thiamine metabolism; Butanoate metabolism; Glycolysis/gluconeogenesis; Porphyrin metabolism. Purine metabolism	Lysine degradation; One-carbon metabolism by folate; Fatty acid biosynthesis	Cultivar-specific tendencies that fine-tune metabolic specialization

Rootstock effects on root metabolomic profiles

Multivariate analysis

PCA of root metabolomes revealed clear multivariate separation among scion–rootstock combinations along the first two ordination axes (Figure 3a, b). In KB55, rootstock-correlated clustering was apparent along Dim1 (36.8% of variance explained) and Dim2 (28.7%), suggesting a structured rootstock-associated pattern in belowground metabolic organization. In MP, Dim1 and Dim2 explained 44.5% and 28.8% of variance, respectively, and rootstock clusters showed broader dispersion in ordination space, consistent with a greater degree of root metabolic differentiation across the rootstock gradient in this cultivar. These variance proportions are descriptive summaries of the pooled-sample ordination and are not accompanied by formal significance tests.

Specifically, Z-score-normalized metabolite abundances were analyzed using hierarchical clustering (Figure 3c, d), which created clusters that generally aligned with PCA patterns: roots from both cultivars clustered primarily by rootstock identity, with slightly more distinct inter-rootstock separation in MP than in KB55, resulting in a broader ordination space.

Distance-based descriptive analyses further contextualized these patterns. Mean Bray–Curtis dissimilarity among rootstocks was 0.748 in KB55 and 0.826 in MP; corresponding mean Euclidean distances were 5.04×10^7 and 6.54×10^7, respectively. Inter-cultivar dissimilarity (Bray–Curtis: 0.865; Euclidean: 6.18×10^7) exceeded the within-cultivar rootstock range in both metrics, indicating that scion genotype is associated with greater overall metabolic differentiation than rootstock variation alone. These metrics are presented as descriptive effect sizes without accompanying inferential tests.

Major compound classes associated with rootstocks

Analysis of root metabolome composition indicated that the diversity and distribution of metabolite classes differed markedly among rootstock–cultivar combinations (Table 2), suggesting that the rootstock is associated with distinct biochemical landscapes in the belowground compartment. Among all chemical families, sesquiterpenoids consistently represented the most diverse class. In S- and CM-budded plants, sesquiterpenoid compound richness was two- to threefold higher than in JC- and RL-budded combinations—a pattern observed across both cultivars and consistent with a strong rootstock-associated effect on terpene-based root metabolism.

Triterpenoids and steroidal derivatives were more numerous in specific rootstock–cultivar combinations, particularly in MP/JC, where five triterpenoid/steroidal compounds were detected, compared with fewer than three in most other combinations. Phenylpropanoid-related metabolites, notably coumarins and their derivatives, were detected across all treatments but showed marked variation in compound richness, with the highest numbers in V- and CM-budded plants. Quinones and lipid-derived metabolites were sparsely represented, appearing only in selected rootstock contexts. Taken together, these patterns indicate that rootstock identity is associated with substantial differences in the functional-class composition of root metabolomes in citrus (Table 2; Figure 3c, d).

Table-2. Compound class abundance in the roots of *Citrus reticulata* cv. Keprok Batu 55 and *Citrus sinensis* cv. Manis Pacitan budded onto five contrasting rootstocks.

Compound Class	Keprok Batu 55					Manis Pacitan				
	JC	RL	V	S	CM	JC	RL	V	S	CM
1. Coumarins & derivatives	2	3	4	1	2	4	3	0	1	4
1. Flavonoids/flavonoid-like compounds	1	1	1	1	1	1	1	0	0	1
3. Quinones	0	1	0	0	0	0	0	0	0	0
4. Monoterpenoids	1	1	1	1	1	1	1	0	1	1
5. Sesquiterpenoids	4	3	6	10	4	5	4	1	9	9
6. Diterpenoids (gibberellin-related)	1	1	0	0	0	0	1	0	0	0
7. Limonoids (triterpenoid derivatives)	1	1	1	0	0	1	1	0	0	1
8. Triterpenoids & steroidal derivatives	3	2	3	1	1	5	2	0	1	1
9. Fatty acids & lipid derivatives	1	0	0	1	0	1	0	0	0	1

https://doi.org/10.35495/ajab.2026.044

Note: Compound-class abundance in the roots of *Citrus reticulata* cv. Keprok Batu 55 and *Citrus sinensis* cv. Manis Pacitan budded onto five contrasting rootstocks. Values represent the number of unique metabolites detected per chemical class, as determined by GC–MS profiling. Rootstocks include Japansche Citroen (JC), Rough Lemon (RL), Volkameriana (V), Salam (S), and Cleopatra Mandarin (CM).

Functional interpretation of root metabolic profiles

Functional annotation of root metabolites suggested that different rootstocks are associated with contrasting belowground chemical profiles that may reflect divergent defense-related or ecological strategies (Figure 3c, d). Metabolites with reported roles in pathogen resistance, rhizosphere interactions, and stress signaling—including sesquiterpenoids, coumarins, quinones, and steroid-derived or oxylipin-related compounds—formed consistent compositional modules that distinguished rootstocks in ordination space. The associations described here are exploratory; no direct bioassay evidence for defensive activity was generated in the present study.

Two broad metabolic profiles were discernible. The S and CM rootstocks were associated with higher compound richness in sesquiterpenoids, prenylated coumarins, furocoumarins, and steroid-like metabolites—classes linked to antifungal and antimicrobial activity in roots of other plant species. The V and RL rootstocks, by contrast, were associated with profiles enriched in oxygenated terpenes, long-chain alcohols, quinone derivatives, and lipid-derived metabolites—classes associated with redox homeostasis and oxylipin signaling in other systems. These contrasting profiles suggest two tentative functional categories: a constitutive chemical-enrichment-oriented profile (S, CM) and a signaling- or redox-oriented profile (V, RL). These interpretations require validation through targeted biochemical and functional studies before conclusions about root defense capacity can be drawn.

Cross-organ metabolomic relationships

Comparison of root and leaf metabolomic patterns across scion–rootstock combinations revealed a degree of inter-organ consistency in the organization of metabolic profiles. Rootstocks associated with higher sesquiterpenoid, coumarin, and steroid compound richness in roots (S, CM; Section 2.2–2.3) corresponded to leaf metabolomes with relatively higher proportions of phenylpropanoids, terpenoids, and sterols—most clearly in KB55 (Section 1.2). Conversely, rootstocks associated with oxygenated-terpene and redox-enriched root profiles (V, RL) corresponded to leaf metabolomes with higher proportions of carbohydrate-interconversion metabolites, NAD-related pyridines, and redox-associated organic acids—most clearly in MP/CM and MP/V. These cross-organ alignments are based on exploratory comparisons of pooled metabolomic data and should not be interpreted as evidence for specific inter-organ signaling mechanisms without further experimental support.

The observed concordance between root and leaf metabolic patterns is consistent with the interpretation that rootstock identity is associated with coherent metabolic profiles spanning both organ compartments, and that scion genotype may modulate the expression of these patterns in a cultivar-specific manner. These patterns point to potential coordination of source–sink relationships and metabolic partitioning across the whole plant in response to rootstock–scion compatibility. This interpretation is speculative and warrants systematic investigation using replicated individual-sample designs with appropriate multivariate integration statistics (e.g., multiblock PCA, O2PLS, or canonical correlation analysis).

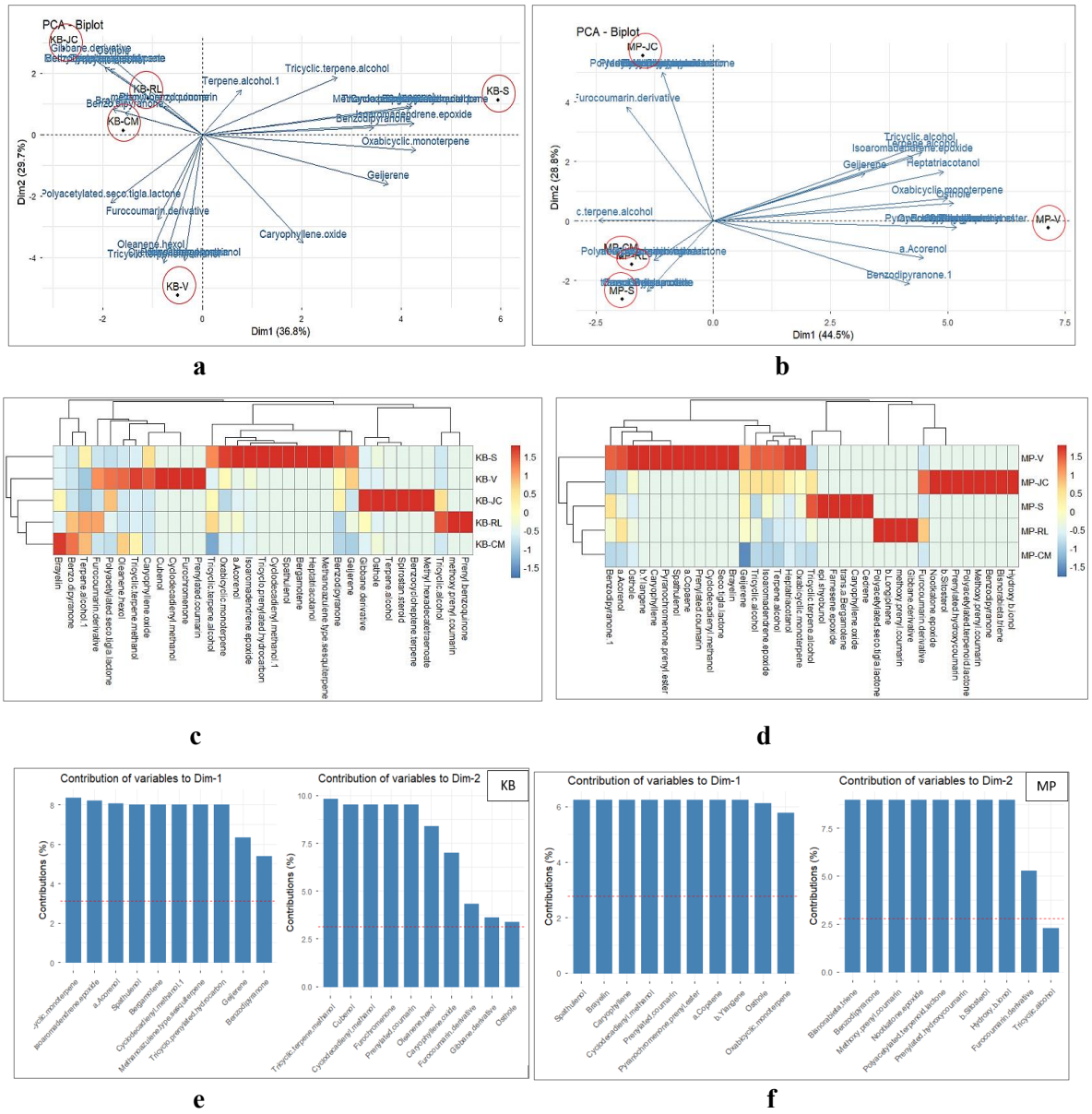

Figure-3. Multivariate differentiation of citrus root metabolomes in *Citrus reticulata* cv. Keprok Batu 55 (KB) (a), and *Citrus sinensis* cv. Manis Pacitan (MP) (b) budded onto five rootstocks (JC, RL, V, S, CM); Hierarchical clustering heatmaps of Z-score-normalized metabolite abundances in KB (c), and MP (d). Contributions of key metabolites to Dim1 and Dim2 in KB (e) and MP (f).

Rootstock effects on leaf anatomical traits

Leaf anatomical traits varied significantly among scion–rootstock combinations, demonstrating strong rootstock control over structural plasticity (Table 3). MP/CM developed the thickest lamina (464.6 µm), whereas KB55/S exhibited the most significant palisade thickness (76.6 µm). Differences in secretory gland size were clearly scion-specific: Scions of KB55 produced cavities 47% larger than those of MP, with combinations of KB55/S and KB55/CM being the largest (>198 µm). We found distinct scion × rootstock interactions with stomatal density, ranging from 443.7 mm^{-2} in KB55/JC to 712.5 mm^{-2} in MP/JC. Microscopic observations (Figure 4a–d) corroborated this quantitative trend, revealing divergent anatomical patterns: increased mesophyll development in KB55/S and lamina thickening with expanded spongy tissue in MP/CM.

Table-3. Leaf anatomical traits (mean ± SD) of citrus scion–rootstock combinations grown under highland conditions.

Treatments	Leaf Thickness (µm)	Upper Epidermis (µm)	Lower Epidermis (µm)	Palisade Thickness (µm)	Ø Secretory Gland (µm)	Stomata Density (mm^2)
KB-CM	319.5 ± 11.0^{e}	11.2 ± 0.5^{e}	13.6 ± 0.8^{a}	58.6 ± 3.2^{de}	198.3 ± 5.5^{a}	618.7±8.6^{c}
KB-JC	355.3 ± 2.3^{d}	16.1 ± 0.9^{abc}	12.7 ± 0.7^{abcd}	69.1 ± 4.1^{bc}	151.9 ± 3.4^{c}	443.7±8.6^{g}
KB-RL	293.8 ± 9.6^{f}	13.9 ± 1.1^{d}	11.6 ± 0.5^{de}	56.7 ± 2.2^{e}	149.7 ± 1.1^{c}	506.2±8.6^{f}
KB-S	397.0 ± 3.2^{b}	17.6 ± 0.6^{a}	12.2 ± 0.3^{bcd}	76.6 ± 1.0^{a}	198.4 ± 17.6^{a}	506.2±8.6^{f}
KB-V	374.9 ± 1.0^{cd}	15.9 ± 1.1^{bc}	10.9 ± 0.6^{e}	73.6 ± 3.0^{ab}	173.4 ± 5.3^{b}	534.4±13.1^{e}
MP-CM	464.6 ± 5.5^{a}	16.3 ± 0.4^{abc}	13.2 ± 0.5^{ab}	54.1 ± 5.1^{e}	108.4 ± 4.4^{d}	584.4±8.6^{d}
MP-JC	387.5 ± 10.4^{bc}	14.7 ± 0.7^{cd}	12.8 ± 0.2^{abc}	56.6 ± 2.0e	83.1 ± 5.4^{e}	712.5±8.6^{a}
MP-RL	366.5 ± 14.9^{d}	16.3 ± 1.0^{abc}	12.0 ± 0.5^{cd}	66.4 ± 2.3^{c}	140.7 ± 8.0^{c}	631.3±8.6^{bc}
MP-S	400.3 ± 7.1^{b}	17.0 ± 0.5^{ab}	13.1 ± 0.4^{abc}	64.6 ± 3.8^{cd}	120.2 ± 3.5^{d}	646.9±8.6^{b}
MP-V	333.6 ± 16.7^{e}	15.5 ± 0.9^{bc}	12.3 ± 0.4^{bcd}	56.9 ± 0.6^{e}	141.0 ± 3.4^{c}	615.6±8.6^{c}

Note: Different letters within a column indicate statistically significant differences among treatments *3.4. Growth and Biomass Allocation Reflect Rootstock–Scion Interactions*.

Growth of ascribed metabolic strategies was consistent with expectations (Figure 4e- i). The tallest plant (KB55/V, 173.3 cm) had the heaviest shoot weight of 729 g, reflecting strong ortholog representation in carbohydrate-related pathways. In contrast, MP and JC, as well as all Salam combinations, showed significantly reduced growth, consistent with the lower-activity profiles assigned by multivariate and pathway analyses. Differences in whole-plant vigor were also reflected by variation in rootstock base diameter, with KB55/V producing the most robust base (24.2 mm). In contrast, scion diameter varied little among treatments, suggesting that rootstock dominance primarily controlled whole-plant vigor. Taken together, these results suggest that the rootstock-mediated metabolic layout is strongly associated with biomass production and structural development, thereby contributing to an integrated view of metabolism and phenotypic performance.

Integration of metabolomic, anatomical, and growth responses

To further interpret the relationships among datasets, patterns observed in metabolomic profiles were compared with variation in anatomical traits and growth performance across scion–rootstock combinations. Rootstocks associated with higher relative abundance of carbohydrate- and redox-related metabolites (e.g., Volkameriana and Rough Lemon) were generally linked to greater vegetative growth and larger biomass accumulation. In contrast, rootstocks associated with higher representation of secondary metabolites, particularly terpenoids and phenylpropanoids (e.g., Salam and Cleopatra mandarin), were associated with increased structural investment in leaf tissues, including greater lamina thickness and modified mesophyll organization.

Although these relationships were not formally tested using correlation statistics due to the use of pooled metabolomic samples, the consistent alignment of metabolic patterns with anatomical and growth traits across treatments suggests coordinated system-level associations. These observations support the interpretation that variation in metabolomic composition may be linked to differences in structural plasticity and growth performance among scion–rootstock combinations.

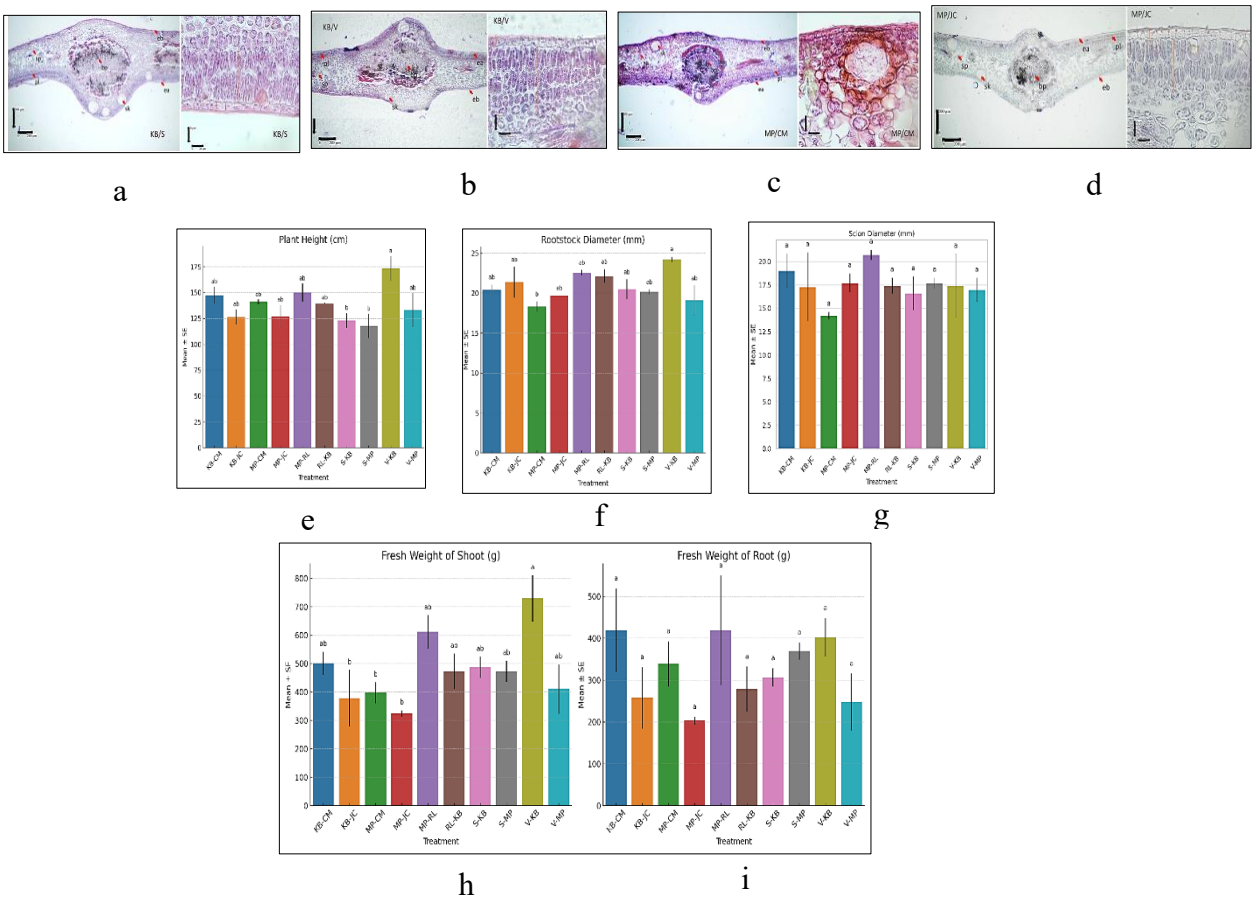

Figure-4. Leaf anatomical cross-sections of citrus scion–rootstock combinations and growth and biomass allocation. Transverse sections are shown for KB–S (a); KB–V (b); MP–CM (c); MP–JC (d); plant height (e); rootstock diameter (f); scion diameter (g); shoot (h) and root (i) fresh weights.

Notes: Anatomical structures are labeled as follows: upper epidermis (ea), lower epidermis (eb), palisade layer (pl), spongy parenchyma (sp), vascular bundle (bp), and secretory cavity (sk). Scale bar = 200 µm (left panels) and 20 µm (right panels). Bars represent mean values ± standard error (SE, n = 3). Different letters above bars indicate statistically significant differences among treatments, as determined by ANOVA followed by Tukey's HSD at $p < 0.05$. Treatments sharing the same letter are not significantly different. Bars represent mean values ± SE (n = 3). Different letters above bars indicate statistically significant differences among treatments, as determined by ANOVA followed by Tukey's HSD at $p < 0.05$.

Discussion

The principal findings indicate that rootstock identity is broadly associated with coordinated patterns of metabolite variation across both organ compartments, that these patterns can be grouped into two functionally contrasting metabolic configurations, and that scion genotype modulates the degree and direction of these patterns' expression at the cultivar level. Furthermore, leaf anatomical traits and growth performance were broadly aligned with these metabolomic configurations, consistent with a system-level integration of metabolic and structural processes across scion–rootstock combinations.

These findings extend a growing body of evidence demonstrating that rootstock effects on scion physiology are mediated by coordinated long-distance signals rather than by modulation of isolated traits (Warschefsky et al., 2016; Notaguchi and Okamoto, 2015). Previous studies have largely focused on effects of rootstock on discrete physiological parameters under a single targeted abiotic or disease treatment, such as water use efficiency, tissue nutrient concentrations, metabolism or stress tolerance (Mesquita et al., 2016; de Souza et al., 2017; Oustric et al., 2021) yet revealed for this work new insights related to the literature through a chloroplast system level where a whole plant context by integrating

metabolic variation into individual organs is one of the characteristics nature of rootstock–scion interactions.

Rootstocks are associated with conserved metabolic frameworks modulated by scion genotype

The primary axis of metabolomic variation in leaf and root metabolomes was associated with rootstock identity rather than scion genotype, across both *Citrus reticulata* cv. Keprok Batu 55 (KB55) and *Citrus sinensis* cv. Manis Pacitan (MP). Rootstock effects on scion gene expression and phytohormone balance at the phytohormone level have been reported (Tardivo et al., 2025), but no systematic metabolome-wide characterization has yet been performed across root and leaf compartments within the same plant—thereby establishing a cross-organ, cross–organ class approach in this study.

KB55 represented relatively higher proportions of phenolics, terpenoids, and sterols, while MP had more modulation on carbohydrate- and NAD-pyridine-class metabolites, respectively. This cultivar-level modulation is consistent with previous evidence indicating that scion genotype regulates flux through the phenylpropanoid pathway via transcriptional and post-transcriptional factors (e.g., MYB transcription factors and miRNA-mediated regulation) (Ninkuu et al., 2025).

Contrasting metabolic configurations reflect alternative strategies of growth–defense allocation

Two contrasting metabolic configurations were observed across scion–rootstock combinations, corresponding to a defense-enriched profile (associated with Salam and Cleopatra Mandarin rootstocks) and a growth-supportive, redox-flexible profile (associated with Volkameriana and Rough Lemon rootstocks). The higher relative abundance of sesquiterpenoids, coumarins, steroidal derivatives, and oxylipin-related metabolites in roots, together with phenylpropanoid- and sterol-rich profiles in leaves, may be in line with investment in constitutive chemical defense and oxidative protection. Sesquiterpenoids, coumarins, and limonoids are the most relevant classes of established citrus secondary metabolites for antimicrobial and antifungal activity (Anjali et al., 2023; Elshafie et al., 2023; Afzal et al., 2025). Conversely, both steroidal and triterpenoid derivatives present at higher abundance in MP/ JC root profiles (Supplementary Figure S8) are associated with sapogenin-related pathways known to enhance antifungal defense in roots of other Rutaceae as well as membrane stabilization (Afzal et al., 2025).

In grafted perennials, enhanced phloem carbon export and sink activity related to carbohydrate pathway enrichment — in particular galactose, fructose, mannose, and starch–sucrose metabolism (Dumont and Rivoal, 2019). The greater levels of NAD-related pyridines in MP are compatible with increased redox cycling capacity via NAD(P)H and promote ROS scavenging, as well as adaptive responses to oxidative stress (Boscari and Frendo, 2025). In V- and RL-associated root profiles, the greater abundance of oxygenated terpenes and lipid-derived metabolites can be attributed to oxylipin biosynthetic activity and a higher level of terpenoid accumulation (Zhang et al., 2019; He et al., 2020). Here, we expand this observation by showing, for the first time for citrus, that rootstock-associated metabolic strategies are systematically expressed in both root and leaf compartments.

Root metabolite profiles suggest rootstock-dependent rhizosphere strategies

The root exudate metabolome is a major component of rhizosphere chemistry in citrus, modulating soil microbial community structure, pathogen resistance, and nutrient availability (Qu et al., 2024; Sorty et al., 2025). That the excess sesquiterpenoid richness in S- and CM-budded plants (two- to threefold more than JC and RL combinations) contrasts with the notably low sesquiterpenoid diversity seen in V- and RL-associated profiles mirrors the contrasting aboveground metabolic profiles above. We identified limonoids, known triterpenoid derivatives specific to Rutaceae (Anjali et al., 2023), in JC and RL root profiles but not in V and S combinations, suggesting that these compounds, characteristic of Rutaceae, were preferentially allocated to roots by the rootstock.

Cultivar-dependent differences in root metabolite diversity were also apparent. MP exhibited higher compound richness overall and broader Bray–Curtis dissimilarity across rootstocks (0.826 vs. 0.748 in KB55), suggesting greater metabolic plasticity in its root response to contrasting rootstock genotypes. KB55, in contrast, showed a more constrained root profile enriched in specific terpenoid classes, consistent with a more canalized belowground chemistry. This difference between cultivars in the degree of root metabolic plasticity parallels the

aboveground findings and reinforces the interpretation that scion genotype modulates the breadth of the whole-plant response to rootstock variation. These findings confirm and extend previous reports of scion-dependent differences in graft-mediated metabolic outcomes (Warschefsky et al., 2016) and specifically point to root metabolite class diversity as a dimension of rootstock–scion compatibility that has not been systematically examined in citrus.

Rootstock-associated metabolic patterns are mechanistically linked to leaf anatomical architecture

The significant variation in leaf anatomical traits across scion–rootstock combinations—including lamina thickness, palisade layer development, secretory gland diameter, and stomatal density—adds a structural dimension to the metabolomic patterns described above and strengthens the case for an integrated rootstock effect on scion development. Crucially, the directionality of anatomical variation was broadly consistent with the metabolomic configurations: combinations associated with defense-enriched metabolic profiles (e.g., KB55/S, MP/CM) showed greater structural investment in leaf tissues, while those associated with growth-supportive profiles (e.g., KB55/V, MP/JC) showed comparatively lower lamina thickness but higher stomatal density.

Mechanistically, matching phenylpropanoid and terpenoid enrichment of leaf metabolomes with increased lamina thickness is consistent with reported structural roles for these classes of compounds in cell wall reinforcement and maintenance of tissue structure. Lignin is a major component of the phenylpropanoid polymer that reinforces the secondary cell wall, regulates water transport via the apoplast, and indirectly protects against pathogen infection by providing an additional physical barrier (Ninkuu et al., 2025). The increased stomatal density of MP/JC could allow for higher gas conductance as well as increase transpiration demand, thereby challenging the ability of carbon assimilation and water use to remain a tradeoff characteristic observed in various stomatal function studies (Bertolino et al., 2019; Haworth et al., 2023). Such patterns indicate that rootstocks are involved in differences in scion developmental trajectories beyond the transport of water and nutrients. Evidence for rootstock-mediated variation in scion performance has comprised variations in hydraulic resistance and xylem properties, which would influence the water transport efficiency of the whole plant and stress resilience (Miranda et al., 2024; Rossdeutsch et al., 2021).

In particular, unsaturated fatty acids, derivatives of lipids, also serve critical functions in stabilizing membranes, maintaining redox equilibria, and mediating stress signaling; thereafter, they serve as precursors for various bioactive molecules, such as jasmonates (He et al., 2020). Those patterns conform to metabolic changes at redox balance and to stress-triggered osmolyte accumulation, which are known to be the main players in plant adaptation to environmental constraints (Dumont and Rivoal, 2019; Franco-Navarro et al., 2025; Boscari and Frendo, 2025). Higher levels of secondary metabolites (especially phenolics and terpenoids) may affect leaf thickness and improve mesophyll organization, thereby enhancing structural reinforcement (Gautier et al., 2019), membrane stability, and antioxidant protection. Such opposing metabolic preferences corroborate alternative strategies that balance growth with defensive functions.

Cross-organ metabolic coordination as a systems-level feature of rootstock–scion interactions

A coherent feature of the dataset is the broadly parallel organization of root and leaf metabolomic profiles across rootstock–scion combinations—rootstocks associated with defense-enriched root chemistry were correspondingly associated with phenylpropanoid- and terpenoid-rich leaf profiles, while rootstocks associated with redox- and signaling-oriented root metabolomes corresponded to carbohydrate- and NAD-pyridine-enriched leaf profiles. This cross-organ consistency is most parsimoniously interpreted as evidence for coordinated whole-plant metabolic responses to rootstock identity that operate across the root-to-shoot continuum.

The graft junction represents the primary interface through which long-distance coordination between rootstock and scion is mediated. Several classes of mobile signals have been identified in grafted plants, including phytohormones (auxin, cytokinin, abscisic acid, gibberellins), mobile proteins and small RNAs, and metabolites transported in the phloem and xylem streams (Notaguchi and Okamoto, 2015). In citrus, specifically xylem-transported abscisic acid is involved in rootstock-mediated stomatal regulation and stress responses (Mesquita et al., 2016;

Rossdeutsch et al., 2021), and phloem-mobile mRNAs have been shown to traverse graft junctions, influencing scion growth (Notaguchi and Okamoto, 2015). The metabolomic coherence observed here is consistent with such a signaling-mediated coordination model, in which rootstock-derived signals traveling through the graft junction reconfigure scion metabolism in a rootstock-specific manner. However, since neither phytohormone flux nor mobile RNA profiles were measured in the present study, this interpretation remains mechanistically inferred rather than directly demonstrated.

The cross-organ patterns observed here are also consistent with a source–sink perspective on graft-mediated metabolic integration. Rootstocks that support higher carbohydrate export and phloem loading (V, RL) would be expected to sustain more vigorous sink activity in the scion, promoting leaf expansion, cell division, and stomatal differentiation—consistent with the growth and anatomical data described above. In contrast, rootstocks that invested more in the root secondary metabolism (S, CM) may have had a bigger carbon flux towards sesquiterpenoid, coumarin, and steroidal compounds in roots at the expense of scion growth; this is consistent with the detrimental effect on growth observed by S budded combinations for both cultivars. In comparison with other grafted crop systems, the degree of cross-organ metabolomic coherence observed in citrus appears broadly consistent with patterns in melon (Zhang et al., 2019), where rootstock identity was also associated with coordinated shifts across multiple metabolic classes in both root and shoot compartments. The citrus-specific contribution of the present study lies in the documentation of this coordination across a wider range of metabolite classes and chemical diversity—particularly the contrast in sesquiterpenoid richness, coumarin deployment, and carbohydrate pathway emphasis across rootstocks with distinct growth characteristics—providing a more comprehensive chemical portrait of rootstock–scion metabolic integration than has been previously reported in *Citrus*.

Metabolic syndromes as a conceptual basis for interpreting HLB-related tolerance through whole-plant integration

Although Huanglongbing (HLB) incidence was not directly quantified in this study, the metabolomic configurations identified here are relevant to the current understanding of how rootstock selection may influence HLB resilience in commercial citrus production. HLB, caused by the phloem-restricted bacterium *Candidatus* Liberibacter asiaticus (CLas), disrupts phloem function, induces systemic oxidative stress, and impairs carbohydrate partitioning and mineral nutrition across the whole plant (Tardivo et al., 2025).

From a metabolic perspective, CLas infection is characterized by extensive perturbation of phenylpropanoid metabolism, accumulation of leaf starch as a source, impaired phloem export—phenotypes that converge on limited carbon supply to sink tissues and systemic redox imbalance (Ninkuu et al., 2025). The defense-boosted metabolic signature of KB55/S and KB55/CM—comprised qualitatively by elevated terpenoid, foliar phenylpropanoid amplification, higher levels of root sesquiterpenoids as well as greater coupling to coumarin-rich metabolites over multiple connections—is consistent with constitutive investment into pre-existing cohorts that CLas actively dismantled or guided toward overexpression. In fact, the activation of the phenylpropanoid pathway (lignin, flavonoids, hydroxycinnamic acids) is one of the first and most characteristic stress responses to infections with phloem-restricted pathogens and is involved in vascular reinforcement and ROS neutralization (Ninkuu et al., 2025). In contrast, the metabolic configuration supporting growth (V, RL rootstocks; especially in MP) has a high capacity for carbon pathways and NAD-linked redox flexibility, which may increase tolerance to HLB-induced phloem dysfunction through alternative carbon routing and oxidative stress management. Retention of capacity for carbohydrate interconversion (galactose, fructose, mannose, and starch–sucrose pathways) and NAD(P)H-linked redox cycling supports viable metabolic strategies that maintain tree vigor, even when successor phloem transport is impaired (Boscari and Frendo, 2025; Alam et al., 2025).

Together, these configurations suggest that citrus tolerance to HLB can be achieved by at least two contrasting metabolic strategies: constitutive chemical fortification (KB55/S and KB55/CM profiles) or metabolic flexibility and growth maintenance (MP/V and MP/RL profiles) at the whole-plant level. This aligns with clinical and field observations that distinct rootstock–scion combinations have different pathways of HLB symptom development and loss of tree

productivity (Tardivo et al., 2025). There is increasing evidence also for rootstock-dependent regulation of reactive oxygen species homeostasis and phytohormone balance, most notably jasmonate and salicylate signaling (Wang et al., 2019), as additional determinants of CLas tolerance; mechanisms that would be consistent with the oxylipin- and NAD-pyridine-associated metabolic patterns noted here.

It is essential to note that all HLB-related interpretations in this section are necessarily indirect. The study was not designed as a disease trial; the CLas infection status of plant material was not assessed, and no direct measurements of pathogen titer, symptom severity, or disease progression were made. The connections drawn between the metabolic configurations described here and HLB-associated biochemical processes are inferential, based on convergence with the broader literature. These interpretations should be considered hypothesis-generating rather than predictive, and validation through integrated studies combining replicated metabolomics, pathogen inoculation, and functional measurements remains essential.

Conclusion

This study demonstrates that citrus rootstocks are associated with distinct metabolomic patterns expressed across both roots and leaves, which are further linked to variation in leaf anatomical traits and vegetative growth. These coordinated patterns suggest that scion–rootstock combinations can be interpreted as integrated systems in which metabolic variation reflects alternative strategies balancing growth, redox regulation, and defense-related processes.

The integration of metabolomic, anatomical, and growth data provides a whole-plant perspective on how rootstock identity is associated with functional variation in citrus, extending beyond single-trait interpretations commonly used in rootstock evaluation.

These findings offer a conceptual basis for interpreting rootstock-associated responses under complex field conditions, including potential relevance to stress resilience such as HLB, although direct validation under disease conditions is required.

Given that metabolomic data were derived from pooled samples, the relationships identified here should be considered exploratory, and future studies incorporating replicated metabolomics and functional validation will be necessary to confirm these associations.

Acknowledgments

We are grateful to ACIAR for providing the funding, and the Research Organization for Agriculture and Food, National Research and Innovation Agency of Indonesia, for supporting this manuscript through internal verification.

Disclaimer: None.

Conflict of Interest: The authors declare that there are no conflicts of interest regarding the publication of this manuscript. In addition, the authors have entirely observed ethical issues, including plagiarism, informed consent, misconduct, data fabrication and/or falsification, double publication and/or submission, and redundancy.

Source of Funding: This study was financially supported by ACIAR HORT 2019/164.

Ethical Approval Statement

We ensure that all research carried out is kept confidential and ethical, and upholds integrity and honesty within the academic community.

Use of Generative AI Tools Statement

While preparing this work, the author(s) used QuillBot, ChatGPT -4, and Claude-3.5 Sonnet to check Grammar and paraphrase. Following the use of this tool/service, the author(s) edited and reviewed the content as necessary and take full responsibility for the content of their publication.

Contribution of Authors

Devy NF, Widyaningsih S, Subandiyah S & Hardiyanto: Conceptualization, methodology, investigation, formal analysis, validation, supervision, project administration, funding acquisition, writing original draft, writing-review and editing.

Yulianti F, Yusnawan E & Sugiyatno A: Methodology, investigation, formal analysis, supervision, writing original draft, writing-review, and editing.

All authors read and approved the final draft of the manuscript.

References

Abadie C, Lalande J and Tcherkez G, 2022. Exact mass GC–MS analysis: Protocol, database, advantages and application to plant metabolic profiling. Plant Cell Environ. 45: 3171–3183. https://doi.org/10.1111/pce.14407.

Afzal MR, Naz M, Yu Y, Yan L, Wang P, Mohotti J, Hao G-F, Zhou J-J, Chen Z, Zhang L and Wang Q, 2025. Root exudates: The rhizospheric frontier for advancing plant–soil interactions. *Plant Environ. Interact.* 6: 2500611.

Alam P, Faizan M, Arif Y, Azzam MM, Hayat S, Afzal S and Albalawi T, 2025. Reactive oxygen species: balancing agents in plants. Front. Plant Sci. 16:1713590. https://doi.org/10.3389/fpls.2025.1713590

Anjali, Kumar S, Korra T, Thakur R, Arutselvan R, Kashyap AS, Nehela Y, Chaplygin V, Minkina T and Keswani C, 2023. Role of plant secondary metabolites in defense and transcriptional regulation in response to biotic stress. Plant Stress 8:100154. https://doi.org/10.1016/j.stress.2023.100154

Asif A, Iqbal S, Aucique-Perez CE, Leaks K, Balal KR, Mattia M, Chater JM and Shahid MA, 2025. Scion–Rootstock Interactions Enhance Freezing Stress Resilience in Citrus reticulata Through Integrated Antioxidant Defence and Carbon–Nitrogen Metabolic Adjustments. Plants 14 (29): 3029. https://doi.org/10.3390/plants14193029.

Auliya I, Hapsari L and Azrianingsih R, 2019. Comparative study of leaf stomata profiles among different ploidy levels and genomic groups of bananas (Musa L.). IOP Conf. Ser. Earth Environ Sci. 391: 012037. https://doi.org/10.1088/1755-1315/391/1/012037.

Balfagón DF, Terán, de Oliveira TDR, Catarina CS and Cadenas AG, 2022. Citrus rootstocks modify scion antioxidant system under drought conditions. Plant Cell Rep. 41: 593-602. https://doi.org/10.1007/s00299-021-02744-y.

Bennici S, Las Casas G, Distefano G, Gentile A, Lana G, Guardo MD, Nicolosi E, Malfa LS and Continella A, 2021. Rootstock affects floral induction in citrus, engaging the expression of the *FLOWERING LOCUS T (CiFT)*. Agriculture 11:140. https://doi.org/10.3390/agriculture11020140.

Bertolino LT, Caine RS and Gray JE, 2019. Impact of stomatal density and morphology on water-use efficiency in a changing world. Front. Plant Sci. 10: 225. https://doi.org/10.3389/fpls.2019.00225

Boscari A and Frendo P, 2025. Redox metabolism and signalling in plants. J. Exp. Bot. 76 (13): 3629–3633. https://doi.org/10.1093/jxb/eraf267

BPS, 2023. Statistical Yearbook of Indonesia, Badan Pusat Statistik Press, Available at www.bps.go.id.

de Souza DJ, de Andrade Silva EM, Coelho Filho MA, Morillon R, Bonatto D, Micheli F and Gesteira ADS, 2017. Different adaptation strategies of two citrus scion/rootstock combinations in response to drought stress. PLoS ONE 12(5): e0177993. https://doi.org/10.1371/journal.pone.0177993

Devy NF, Subandiyah S, Widyaningsih S, Hardiyanto, Yulianti F, Agisimanto D, Sugiyatno A and Dwiastuti ME, 2023. The effect of rootstocks on morphological, physiological, and gene expression characters of citrus seedlings grown under drought conditions. Hortic. Sci. (Prague) 51(4): 255-269. https://doi.org/10.17221/136/2023-HORTSCI

Dumont S and Rivoal J, 2019. Consequences of Oxidative Stress on Plant Glycolytic and Respiratory Metabolism. Front. Plant Sci. 10: 166. https://doi.org/10.3389/fpls.2019.00166

Elshafie HS, Camele I and Mohamed AAA, 2023. Comprehensive Review on the Biological, Agricultural and Pharmaceutical Properties of Secondary Metabolites Based-Plant Origin. Int. J. Mol. Sci. 24: 3266, https://doi.org/10.3390/ijms24043266

Fan R, Zhu C, Qiu D, Mao G, Mueller-Roeber B and Zeng J, 2023. Integrated transcriptomic and metabolomic analyses reveal key genes controlling flavonoid biosynthesis in Citrus grandis 'Tomentosa' fruits. Plant Physiol. Biochem. 196: 210–221. https://doi.org/10.1016/j.plaphy.2023.01.050.

Franco-Navarro JD, Padilla YG, Álvarez S, Calatayud Á, Colmenero-Flores JM, Gómez-Bellot MJ, Hernández JA, Martínez-Alcalá I, Penella C, Pérez-Pérez JG, Sánchez-Blanco MJ, Tasa M and Acosta-Motos JR, 2025. Advancements in water-saving strategies and crop adaptation to drought: A comprehensive review. Physiol. Plant. 177, e70332. https://doi.org/10.1111/ppl.70332

Gautier AT, Chambaud C, Brocard L, Ollat N, Gambetta GA, Delrot S and Cookson SJ, 2019. Merging genotypes: graft union formation and scion-

rootstock interactions. J. Exp. Bot. 70 (3):747-755. http://doi.org/10.1093/jxb/ery422.

Haworth M, Giovanni M, Alessandro M, Antonio R, Charles PS and Mauro C, 2023. The functional significance of the stomatal size to density relationship: Interaction with atmospheric [CO_2] and role in plant physiological behavior. Sci. Total Environ. 863: 160908. http://doi.org/10.1016/j.scitotenv.2022.160908.

Hazrati H, Kudsk P, Ding L, Uthe H and Fomsgaard IS, 2022. Integrated LC–MS and GC–MS-based metabolomics reveal the effects of plant competition on the rye metabolome. *J. Agric. Food Chem.* 70 (9): 3056-3066.

He M, C-X. Qin C-X, Wang X and Ding N-Z, 2020. Plant Unsaturated Fatty Acids: Biosynthesis and Regulation. Front. Plant Sci. 11:390. https://doi.org/10.3389/fpls.2020.00390

He W, Chai J, Xie R, Wu Y, Wang H, Wang Y, Chen Q, Wu Z, Li M and Lin Y, 2024. The Effects of a New Citrus Rootstock *Citrus junos* cv. Shuzhen No. 1 on Performances of Ten Hybrid Citrus Cultivars. Plants 13(6): 794. https://doi.org/10.3390/plants13060794.

He W, Luo L, Xie R, Chai J, Wang H, Wang Y, Chen Q, Wu Z, Yang S, Li M, Lin Y, Zhang Y, Luo Y, Zhang Y, Tang H and Wang X, 2023. Transcriptome sequencing analyses uncover mechanisms of citrus rootstock seedlings under waterlogging stress. Front. Plant Sci. 14: 1198930. https://doi.org/10.3389/fpls.2023.1198930.

Lisec J, Nicolas S, Joachim K, Lothar W and Fernie AR, 2006. Gas chromatography mass spectrometry–based metabolite profiling in plants. Nat. Protoc. 1 (1): 387-396. https://doi.org/10.1038/nprot.2006.59

Liu XY, Li MM, Liu QY and Chen JZ, 2017. Transcriptome Profiling to Understand the Effect of Citrus Rootstocks on the Growth of `Shatangju' Mandarin. PLoS ONE 12(1): e0169897. https://doi.org/10.1371/journal.pone.0169897

Maciá-Vázquez AA, Martínez-Nicolá JJ, Gómez DN, Melgarejo P and Legua P, 2024. Influence of rootstock on yield, morphological, biochemical and sensory characteristics of 'Afourer' variety mandarins. Sci. Hortic. 325:112644. https://doi.org/10.1016/j.scienta.2023.112644

Mesquita GL, Zambrosi FCB, Tanaka FAO, Boaretto RM, Quaggio JA, Ribeiro RV and Mattos-Jr. D, 2016. Anatomical and Physiological Responses of Citrus Trees to Varying Boron Availability Are Dependent on Rootstock. Front. Plant Sci. 7: 224. https://doi.org/10.3389/fpls.2016.00224

Metusala D, 2017. An alternative simple method for preparing and preserving cross-section of leaves and roots in herbaceous plants: Case study in Orchidaceae. AIP Conf. Proc. 1862: 030113. https://doi.org/10.1063/1.4991217

Miranda MT, Pires GS, Pereira L, de Lima RF, da Silva SF, Mayer JLS, Azevedo FA, Machado EC, Jansen SS and Ribeiro RV, 2024. Rootstocks affect the vulnerability to embolism and pit membrane thickness in Citrus scions. Plant Cell Environ. 47:3063–3075. https://doi.org/10.1111/pce.14924

Morade AS, Sharma RM, Dubey AK, Sathee L, Kumar S, Kadam DM, Awasthi OP, Kumar A and Yadav D, 2025. Phenotyping drought stress tolerance in citrus rootstocks using high-throughput imaging and physio-biochemical techniques. BMC Plant Biol. 25: 753. https://doi.org/10.1186/s12870-025-06823-0.

Ninkuu V, Aluko OO, Yan J, Zeng H, Liu G, Zhao J, Li H, Chen S and Dakora FD, 2025. Phenylpropanoids metabolism: recent insight into stress tolerance and plant development cues. Front. Plant Sci. 16: 1571825. https://doi.org/10.3389/fpls.2025.157182

Notaguchi M and Okamoto S, 2015. Dynamics of long-distance signaling via plant vascular tissues. Front. Plant Sci. 6: 161. https://doi.org/10.3389/fpls.2015.00161.

Oustric J, Stéphane H, Yann Q, Raphaël M, Jean G, Liliane B and Jérémie S, 2021. Tetraploid Citrumelo 4475 rootstocks improve diploid common clementine tolerance to long-term nutrient deficiency. Sci. Rep. 11: 8902. https://doi.org/10.1038/s41598-021-88383-5.

Paul V, Sharma L, Pandey R and Meena RC, 2017. Measurements of stomatal density and stomatal index on leaf/plant surfaces. In: Manual of ICAR Sponsored Training Programme on "Physiological Techniques to Analyze the Impact of Climate Change on Crop Plants", IARI. New Delhi.

Putra AM, Anastasya NA, Rachmawati SW, Yusnawan E, Syibli MA, Trianti I, Setiawan A and Aini LQ, 2024. Growth performance and metabolic changes in lettuce inoculated with plant growth promoting bacteria in a hydroponic system. *Sci. Hortic.* 327: 112868.

Qu P, Wang B, Qi M, Lin R, Chen H, Xie C, Zhang, Qiu J, Du H and Ge Y, 2024. Medicinal Plant Root Exudate Metabolites Shape the Rhizosphere Microbiota. Int. J. Mol. Sci. 25 (9): 7786. https://doi.org/ 10.3390/ijms25147786

Razi K, Suresh P, Mahapatra PP, Al Murad M, Venkat A, Notaguchi M, Bae DW, Prakash MAS and Muneer S, 2024. Exploring the role of grafting in abiotic stress management: Contemporary insights and automation trends. Plant Direct 8: e70021. https://doi.org/10.1002/pld3.70021

Rossdeutsch L, Schreiner RP, Skinkis PA and Deluc L, 2021. Nitrate Uptake and Transport Properties of Two Grapevine Rootstocks with Varying Vigor. Front. Plant Sci. 11: 608813. https://doi.org/10.3389/fpls.2020.608813

Sorty AM, Kudjordjie EN, Meena KK, Nicolaisen M and Stougaard P, 2025. Plant root exudates: Advances in belowground signaling networks, resilience, and ecosystem functioning for sustainable agriculture. Plant Stress 17:100907. https://doi.org/10.1016/j.stress.2025.100907

Tardivo C, Pugina G, Bowman KD and Albrecht U, 2025. Field Performance of Novel Citrus Rootstocks Grafted with 'Valencia' Orange and Their Response to Systemic Delivery of Oxytetracycline. Plants 14: 3020. https://doi.org/10.3390/plants14193020

Vives-Peris VJ, Domínguez-Figueroa J, Gómez-Cadenas A and Pérez-Clemente RM, 2023. Morphological, physiological, and molecular scion traits modulated by citrus rootstocks under drought stress. Front. Plant Sci. 14: 1132963. https://doi.org/10.3389/ fpls.2023.1132963.

Wang P, Liu F, Sun Y, Liu X and Jin L, 2025. Physiological and Molecular Insights into Citrus Rootstock–Scion Interactions: Compatibility, Signaling, and Impact on Growth, Fruit Quality, and Stress Responses. Horticulturae 11: 1110. https://doi.org/10.3390/ horticulturae11091110.

Wang S, Alseekh S, Fernie AR, and Luo J, 2019. The structure and function of major plant metabolite modifications. Mol. Plant 12: 899–919. https://doi.org/10.1016/j.molp.2019.06.001.

Wang T, Xiong B, Liping T, Youting Y, Zhang Y, Ma M, Yinghuan Y, Ling L, Guochao S, Dong L, Hui X, Zhang X, Wang Z and Wang J, 2020. Effects of interstocks on growth and photosynthetic characteristics in 'Yuanxiaochun' Citrus seedlings. Funct. Plant Biol. 47(11): 977-987. https://doi.org/10.1071/FP20079.

Warschefsky EJ, Klein LL and Frank MH, 2016. Rootstocks: Diversity, domestication, and impacts on scion phenotypes. Trends Plant Sci. 21: 418–437.

Xie J, Xiong H, Niu R, Wang Y, Lali MN, Zhao J, Shi X and Rennenberg H, 2025. Nutrient acquisition efficient rootstocks improve zinc nutrition of top-budded citrus trees on calcareous soil. Front. Plant Sci. 16: 1615405. https://doi.org/10.3389/fpls.2025.1615405.

Yang L, Li S, Chen Y, Wang M, Yu J, Bai W and Hong L, 2024. Combined metabolomics and network pharmacology analysis reveal the effect of rootstocks on anthocyanins, lipids, and potential pharmacological ingredients of Tarroco blood orange (*Citrus sinensis* L. Osbeck). Plants 13(16): 2259. https://doi.org/10.3390/plants13162259.

Zhang S, Zhao Y and Shi H, 2019. Metabolomic analysis of the occurrence of bitter fruits on budded oriental melon plants. PLoS ONE 14 (10): e0223707. https://doi.org/10.1371/journal.pone.0223707

Zhou H, Wang F, Hong Y, Zhang M, Dong J, Huang T, Xiang J, Zhu S and Zhao X, 2022. Effects of scion-rootstock interaction on citrus fruit quality related to differentially expressed small RNAs. *Sci. Hortic*. 298:110974. https://doi.org/10.1016/j.scienta.2022.110974

Zhu Y, Lulu Q, Zihao W and Pu S, 2024. Spectra-based predictive mapping of soil organic carbon in croplands: Single-date versus multitemporal bare soil compositing approaches. Geoderma 449: 116987. https://doi.org/10.1016/j.geoderma.2024.116987.